Since January 2020 Elsevier has created a COVID-19 resource centre with free information in English and Mandarin on the novel coronavirus COVID-19. The COVID-19 resource centre is hosted on Elsevier Connect, the company's public news and information website.

Chemical Engineering Journal 399 (2020) 125867

Contents lists available at ScienceDirect

Chemical Engineering Journal

journal homepage: www.elsevier.com/locate/cej

Fluorescent linear polyurea based on toluene diisocyanate: Easy preparation, broad emission and potential applications

Hongyan Cao[a,b], Bin Li[a,c], Xubao Jiang[a,*], Xiaoli Zhu[a], Xiang Zheng Kong[a,*]

[a] College of Chemistry and Chemical Engineering, University of Jinan, Jinan 250022, China
[b] College of Chemistry and Chemical Engineering, Dezhou University, Dezhou 253023, China
[c] Québec Center for Functional Materials, Department of Chemistry, Université de Sherbrooke, Sherbrooke, QC J1K2R1, Canada

HIGHLIGHTS

- Toluene diisocyanate (TDI) based polyurea (TPU) is prepared by TDI reaction with H_2O.
- TPU shows strong fluorescent emission as solid powder and in its solution.
- The emission in UV region is intrinsic due to its phenyl and the adjacent urea group.
- The emission in visible zone is owing to the formation of molecule clusters.
- Paper strip dipped in TPU solution is used for easy detections of Fe^{3+} and H_2O_2.

GRAPHICAL ABSTRACT

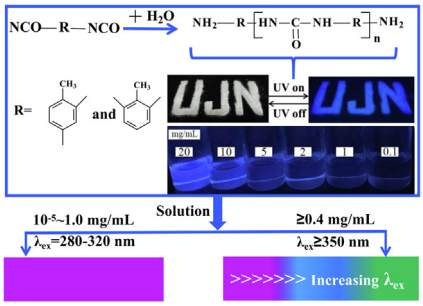

ARTICLE INFO

Keywords:
Polyurea
Precipitation polymerization
Fluorescent emission
Cluster formation
Ferric ion quenching

ABSTRACT

In contrast to conventional fluorescent polymers featured by large conjugation structures, a new class of fluorescent polymers without above conjugations are gaining constant interest owing to their significant academic importance and promising applications in diverse fields. These unconventional fluorescent polymers are in general composed of heteroatoms (e.g. N, O, P, and S) under different forms. Here we report our recent study on polyurea, prepared by a very simple one step precipitation polymerization of toluene diisocyanate in a binary solvent of water-acetone. This polyurea, basically consisting of phenyl ring and urea group, shows fluorescent emission in a broad concentration range, from very low (10^{-5} mg/mL) to its solubility limit (50 mg/mL), and in a wide range of emission wavelength from UV to visible regions of up to 500 nm under varied excitation wavelength. The emission behaviors were fully studied under different concentrations and excitations. It was concluded that the emission in UV region was intrinsic due to the conjugation between the phenyl and the adjacent urea unit; while the emission in visible region, strongly excitation dependent, was caused by the cluster formation of the molecular chains, in accordance with the cluster-triggered-emission (CTE) mechanism. The formation of the cluster was tested through dynamic light scattering, FTIR and UV absorbance. Tested in presence of different metal ions, Fe^{3+} demonstrated a quenching effect with high selectivity. Based on this study, different paper-based sensors were designed to detect Fe^{3+}, H_2O_2 in bioanalysis and for data encryption. This work provides a simple way to prepare a polyurea, a novel type of unconventional fluorescent polymer, with high emission performance distinct from its known analogues.

* Correspondence authors.
E-mail addresses: chm_jiangxb@ujn.edu.cn (X. Jiang), xzkong@ujn.edu.cn (X.Z. Kong).

https://doi.org/10.1016/j.cej.2020.125867
Received 15 April 2020; Received in revised form 8 June 2020; Accepted 9 June 2020
Available online 13 June 2020
1385-8947/

1. Introduction

Fluorescent materials have been a hot topic in fundamental researches since long because of their wide applications in a huge variety of fields, particularly in the fields of optoelectronic devices [1,2], drug delivery, cell imaging and biosensors [3–6] and so forth. Among these studies, fluorescent polymers have gained great significance for the past decades, because of their processability and practically unlimited possibility of functionalization through their preparations and post-modifications. Nowadays a huge amount of studies are being reported for various applications [2–10]. It is to note that, just about two decades ago, a prerequisite to be fluorescent for any organic substances including polymers was that their molecules contain at least one chromophore group, such as cyanine [11], triarylamine [12], pyrazoline [13], carbazole [14], benzoxazole [15], benzothiazole azo [16,17]. The common feature for these materials is that they all contain aromatic building blocks or conjugated structures acting as emitting entities [4–6]. In 2004, the well-known dendrimer, poly(amidoamine) (PAMAM), was reported to exhibit strong fluorescence under appropriate conditions [18,19]. The significance of these reports is that, in contrast to the conventionally common view, this PAMAM contains neither aromatic unit nor conjugated structure. Since then, a large amount of polymers have been found to be fluorescent [5,6], including polysiloxane, poly(amido acid), poly(amino ester), phenolic formaldehyde amine, and polyimine based on propylene, ethylene and propyl ether, which are commonly featured by the absence of traditional/conventional chromophores in their molecules. And instead, these polymers are in generally consisted of heteroatom, electron rich and non-emissive functional groups. As such, this type of new fluorescence is referred to as intrinsic photoluminescence (IPL) [4] or non-traditional intrinsic luminescence [5]. As to the mechanism of this type of fluorescence emission, the cluster-trigged emission (CTE) proposed by Tang et al. [20,21], has been widely accepted, which suggests that the emission is owing to the formation of clusters when the polymer reaches a high concentration, caused by the intra- and interchain interactions of their electron-rich groups by sharing their lone-pair electrons. This CTE mechanism is similar to the AIE mechanism proposed also by these authors earlier [22,23], from the view point that the emission is caused by structural rigidification of their non-emissive moieties, due to the restriction of inter- and intramolecular mobility. The related studies have been well updated by different reviews [3–6].

Polyurea chains are consisting of electron rich urea groups (–NHCONH-) of heteroatoms (O and N) with lone-pair electrons [24–26]. In contrast to the IPL polymers studied, polyurea has been rarely reported for their fluorescence property [27]. We report herein a toluene diisocyanate (TDI) based polyurea (TPU), prepared by step-growth polymerization of TDI in a binary mixture of water–acetone [24,25,28]. This TPU was shown to have typical CTE behavior, and its emission was concentration and excitation dependent. TPU was applied as a chemosensor for Fe^{3+} and H_2O_2. The emission mechanism was thoroughly discussed.

2. Experimental

2.1. Materials

Toluene diisocyanate (TDI, industrial grade, 80% of 2,4- and 20% of 2,6-TDI) was purchased from Beijing Keju New Materials Co. Ltd. and distilled under reduced pressure just before use. N,N′-dimethylenediamine, *p*-tolyl isocyanate, dimethylsulfoxide (DMSO), deuterated DMSO-d_6, hydrogen peroxide (H_2O_2, 30 wt% in H_2O) and all salts used to have ions for emission quenching tests, i.e. $Cd(NO_3)_2{\cdot}4H_2O$, $AgNO_3$, $FeCl_3{\cdot}6H_2O$, $Ni(NO_3)_2{\cdot}6H_2O$, $CuSO_4{\cdot}5H_2O$, $CaCl_2$, $FeCl_2$, $Pb(NO_3)_2$ and CuCl, all AP grade, were purchased from Aladdin Co. Ltd. N-butylamine, ethylenediamine, acetone and acetonitrile were from Tianjin Fuyu Fine Chemicals. Potassium bromide (KBr, SP), 2-phenylethyl amine and 2-phenethyl isocyanate were purchased from Shanghai Macklin Biochemical Co. Ltd. Double distilled water was laboratory-made. All regents were used directly unless otherwise stated.

2.2. Synthesis of polyurea TPU

A mixture of H_2O-acetone (90.0 g) at mass ratio of 3/7 was first charged into a round bottom flask of 250 mL, immersed in a water bath at 30 °C. TDI (10.0 g) was added in at a rate of 20 mL/h under stirring at 300 rpm. The polymerization was allowed to continue for 2 h after TDI addition completed, followed by centrifugation to separate the solid, which was rinsed twice by acetone and dried at 70 °C under vacuum to get a powder product, i.e. the polyurea (TPU, Fig. S1).

2.3. Syntheses of organic urea model compounds

In this study, four model compounds with urea unit were synthesized, and nominated as M1 (by reaction of *n*-butylamine and 2,4-TDI), M2 (by reaction of *p*-toluene isocyanate with water), M3 (by reaction of *n*-butylamine and *p*-toluene isocyanate) and M4 (by reaction of 2-phenethyl isocyanate with 2-phenylethyl amine) (Fig. S2). All syntheses were done at 30 °C with equivalent amounts for all the starting reagents. Taking the synthesis of the compound M3 as an example: *n*-butylamine (0.53 g, 7.2 mmol) was dissolved in acetonitrile (28.58 g) at 30 °C, and *p*-toluene isocyanate (0.96 g, 7.2 mmol) was added in under stirring. The reaction was allowed to proceed for 4 h. The product M3 was seen to precipitate out during the reaction. At end of the synthesis, the reaction mixture was filtrated to separate out the product, which was dried under vacuum at room temperature. The synthesis protocol for the other three compounds was the same, except for M2 where a binary solvent of water/acetonitrile (3/7 by vol.) was used instead of pure acetonitrile.

2.4. Instrumentation and characterization

Chemical structures of the four organic model compounds (M1 to M4) were characterized by ^{1}H NMR (Avance III 400 M, Brüker) in DMSO-d_6 as the solvent. The form of TPU presence state in solutions was estimated by FTIR (Spectrum GX, Perkin-Elmer) by placing a drop of TPU solution on a KBr pallet. UV–vis absorbance spectra of the four organic model molecules, TPU solution and its solid powder were all measured using a Perkin-Elmer spectrophotometer (Lambda 35). The size of the clusters was detected by dynamic light scattering nanosizer (DLS, Nano-ZS 3600, Malvern). Fluorescence emission and excitation spectra of all samples were recorded by a fluorescence spectrometer (F-7000, Hitachi), with both the excitation and emission slit widths of 2.5 nm.

3. Results and discussion

3.1. Fluorescent emission of TPU

The reactions involved in the synthesis of polyurea TPU, by dissolving TDI in the binary mixture of water–acetone, are well known [24,28,29]: in a first step, TDI reacts with water to yield toluene diamine (TDA) with the release of CO_2, the in-situ formed TDA reacts then with TDI to form TPU (Fig. S1). TPU as prepared was characterized in previous studies, which showed that this polyurea was a typical porous material, with the specific surface area of 161.68 m^2/g, the pore volume of 2.20 cm^3/g. The pore size distribution, determined by Hg intrusion and BET tests, was quite broad, with the pore size varied from a few nanometers to dozens of micrometers [29]. TPU was also used for enzyme immobilization and kinetic resolution of racemic molecules [24].

Under mercury lamp (λ_{ex} = 365 nm), the white TPU powder exhibited strong blue emission at room temperature (Fig. 1A). From its excitation spectrum with emission λ_{em} = 440 nm, a maximal

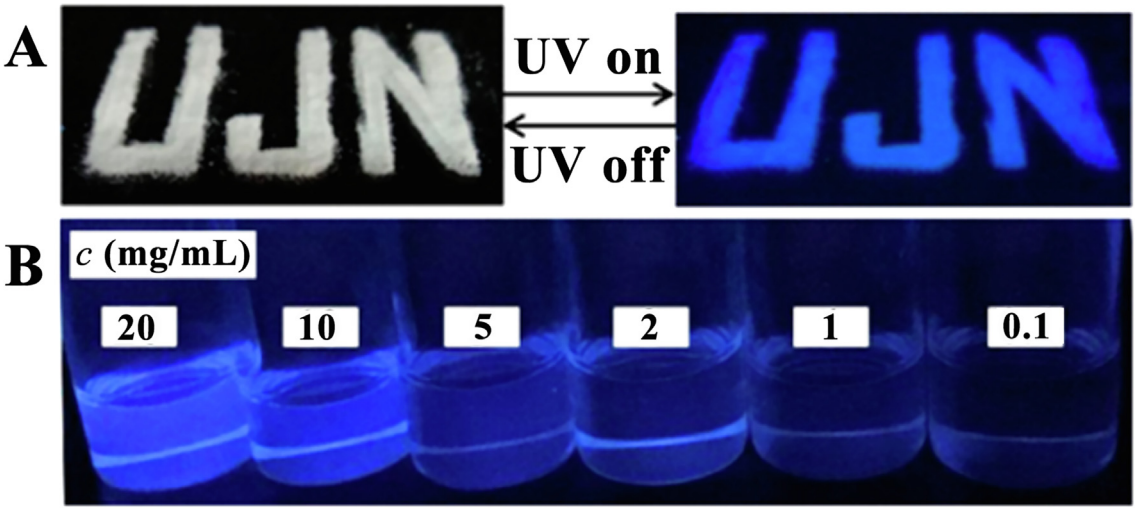

Fig. 1. Photos of TPU powder taken under daylight (A, left) and 365 nm UV irradiation (A, right); Photos of TPU solutions (B) in DMSO at different concentrations under λ_{ex} = 365 nm.

excitation, λ_{ex} = 370 nm, was indeed confirmed (Fig. S3A). In addition, another emission at λ_{em} = 355 nm was also detected at excitation λ_{ex} = 320 nm (Fig. S3B).

Under irradiation of λ_{ex} = 365 nm, TPU solution in DMSO exhibited blue emission, and the emission was enhanced with TPU concentration (Fig. 1B). With different excitation wavelength λ_{ex}, TPU solution was emissive from 10^{-4} to 20 mg/mL, although the emission intensity and its maximal emission wavelength changed with its concentration (Fig. 2). Under excitation of λ_{ex} = 300 nm, the maximal emission of TPU was at 355 nm, detected from a concentration of as low as 10^{-5} mg/mL (Fig. 2A), followed by a sharp increase in emission intensity with the concentration; The emission reached its maximal intensity at 0.05 mg/mL, and declined quickly with the increase in concentration and became non-emissive at 0.4 mg/mL (Fig. 2A, D). With the excitation wavelength increased to λ_{ex} = 320 nm, the maximal emission of TPU remained at 355 nm (Fig. 2B). However, the emission was detectable from 0.01 mg/mL to 5.0 mg/mL, with the maximal intensity observed at 1.0 mg/mL (Fig. 2B, D). That is to say that, with λ_{ex} increased from 300 nm to 320 nm, both the concentration to have the highest emission intensity and the concentration range to be emissive were dramatically changed, though the maximal emission was kept at λ_{em} = 355 nm, the same as λ_{ex} = 300 nm (Fig. 2A). With the excitation wavelength increased further to λ_{ex} = 350 nm (Fig. 2C), the emission at 355 nm disappeared, and instead a new emission appeared at around λ_{em} = 440 nm. In addition, this emission was undetectable at TPU concentration of 0.2 mg/mL and below, started to appear at 0.4 mg/mL with λ_{em} = 438 nm. And a slight red-shift of the emission with concentration was also seen: the maximal emission shifted to λ_{em} = 440 nm at concentration of 2.0 mg/mL, and it shifted further to λ_{em} = 444 nm with the concentration increased to 20 mg/mL (Table S1). It is highly important to note that, this emission under excitation at λ_{ex} = 350 nm was quite different from that at lower excitation (λ_{em} = 355 nm with λ_{ex} at 300 & 320 nm): Not only the emission red-shifted with concentration, but also the absence of the upper limit for TPU concentration vis-à-vis the emission intensity, which was linearly increased with TPU concentration increase up to 50 mg/mL. Above this concentration, emission intensity was practically constant owing to the solubility limit. This was a strong indication that the emission center or species at λ_{ex} = 350 nm must be different from that at excitation with lower wavelength, i.e. with λ_{ex} = 300 and 320 nm.

These results revealed that the emission of TPU solution was significantly dependent on its concentration and excitation. Under short wavelength excitation ($\lambda_{ex} \leq$ 320 nm), it was emissive in UV zone (λ_{em} = 355 nm), the emission was well seen at low concentration ($\leq$0.1 mg/mL), and quickly faded out with increased concentration or excitation wavelength (Fig. 2A, B). Under longer wavelength excitation (λ_{ex} = 350 nm) of a TPU solution with higher concentration ($\geq$0.4 mg/mL), the emission shifted to a higher wavelength in the visible region (λ_{em} around 440 nm). By increasing TPU concentration, the emission was enhanced (Fig. 2C) rather than the inverse observed under shorter wavelength excitation ($\lambda_{ex} \leq$ 320 nm) and at lower concentration ($\leq$0.1 mg/mL). Taking into account of these observations, a TPU solution of 5.0 mg/mL was made, a concentration where emission was detectable under excitation with λ_{ex} at 320 and 350 nm, and its emission was observed under different excitation from λ_{ex} = 320 to 440 nm. From the results given in Fig. 3, it is seen that, under excitation of λ_{ex} = 320 nm, only one single emission was seen in UV zone at λ_{em} = 355 nm; with excitation at λ_{ex} = 325 nm, the emission at 355 nm was intensified, and a new broad and weak emission appeared in the visible region at λ_{em} = 418 nm; with the excitation wavelength increased to λ_{ex} = 330 nm, both the two emissions were distinct, the one at 355 nm was attenuated and that in the visible region (424 nm) boosted up; by shifting further the excitation wavelength to λ_{ex} = 340 nm, the emission at λ_{em} = 355 nm practically disappeared, leaving one single emission in the visible region at λ_{em} = 428 nm. This emission in visible region was in constant red-shifting with increased wavelength of the excitation. By changing excitation from λ_{ex} = 330 nm to 440 nm, the emission red-shifted from λ_{em} = 424 nm to 512 nm (Table S2, Fig. 3), an obvious excitation dependent emission (EDE). It is worth noting that a highest intensity of emission (λ_{em} = 438 nm) was observed at excitation of λ_{ex} = 360 nm, the emission intensity was attenuated with the excitation going to either direction from the mission under excitation λ_{ex} = 360 nm.

3.2. Fluorescence mechanism of TPU

The above results demonstrated clearly that, under short excitation wavelength ($\lambda_{ex} \leq$ 320 nm), TPU emitted in UV zone (λ_{em} = 355 nm), the position of the emission maximum was independent of the excitation wavelength, and the emission disappeared at a given higher concentration. With a longer excitation ($\lambda_{ex} \geq$ 340 nm), TPU emission red-shifted to visible region ($\lambda_{em} \geq$ 428 nm), and the emission was of typical EDE. Based on the studies on fluorescent polymers [5,6,10], we strongly suggest that the emission of TPU in UV zone and that in the visible region came from different emission centers, or these two emissions must be ascribed to different forms of TPU chains. At concentration of 5.0 mg/mL, TPU chains were assumingly present as fully dissolved on one hand, and they might also form clusters on the other

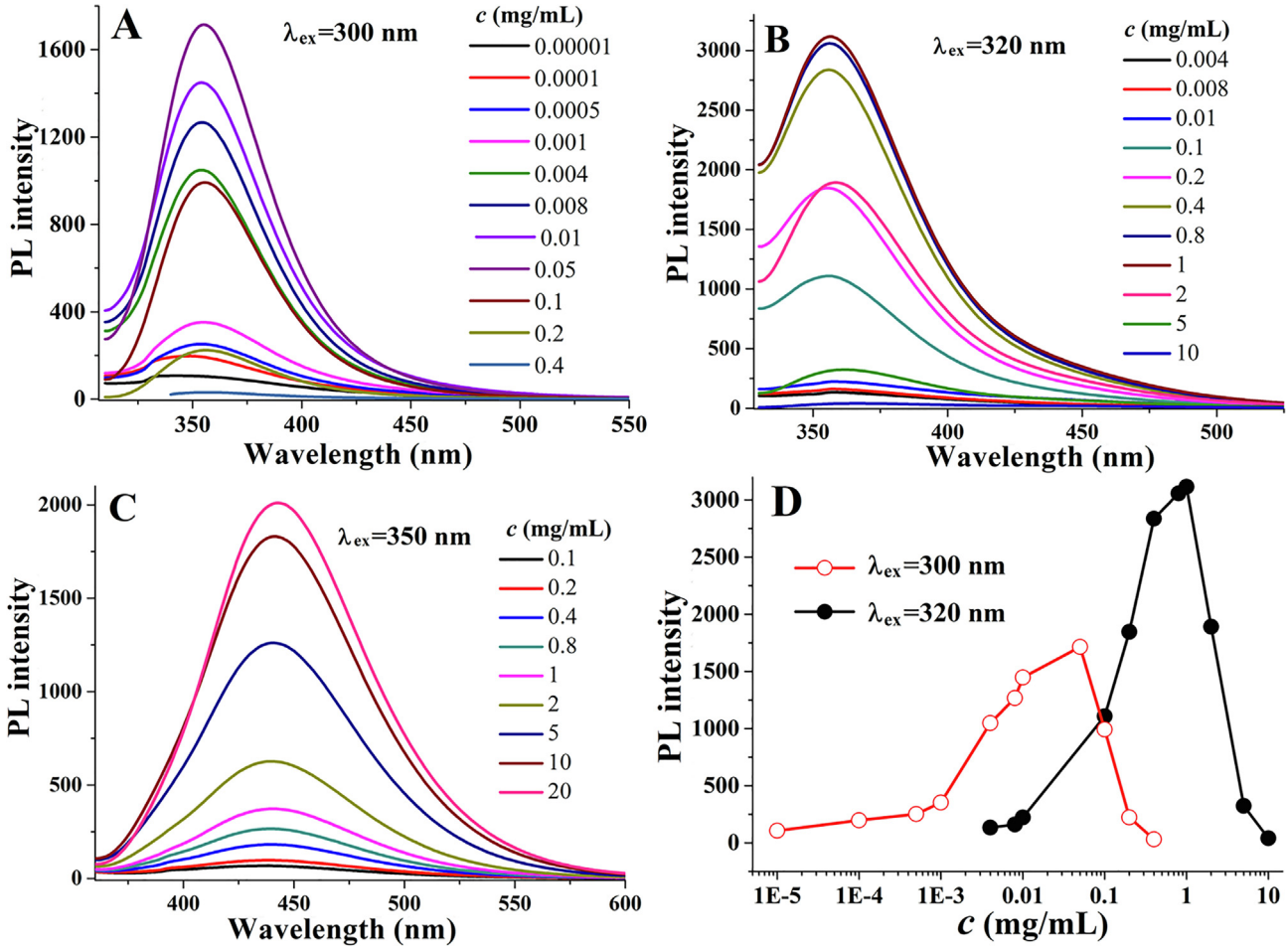

Fig. 2. Fluorescent emission spectra of TPU in DMSO at concentration varied from 10^{-5} to 0.4 mg/mL under λ_{ex} = 300 nm (A); the spectra at concentration from 0.004 to 10 mg/mL under λ_{ex} = 320 nm (B); those at concentration from 0.1 to 20 mg/mL under λ_{ex} = 350 nm (C); Emission intensity as function of TPU concentration from 10^{-5} to 0.4 mg/mL under λ_{ex} = 300 nm (red line), and that from 0.004 to 10 mg/mL under λ_{ex} = 320 nm (black line) (D). (For interpretation of the references to color in this figure legend, the reader is referred to the web version of this article.)

hand. It is conjectured that the emission in UV region at λ_{em} = 355 nm was caused by TPU chains individually dissolved, while the emission in visible region at $\lambda_{em} \geq$ 428 nm was owing to the clustering of TPU chains, suggesting that the EDE in visible region was typical CTE emission as afore-mentioned [20,21].

3.2.1. TPU emission in UV region

As mentioned above, the emission of TPU in its solution ought to come from the molecules themselves when they are dissolved individually in DMSO. Originated from TDI, phenyl rings are present in TPU chains (Fig. S1). Independent benzene ring is believed either non-emissive or to be emissive at λ_{em} = 280 nm with very low intensity

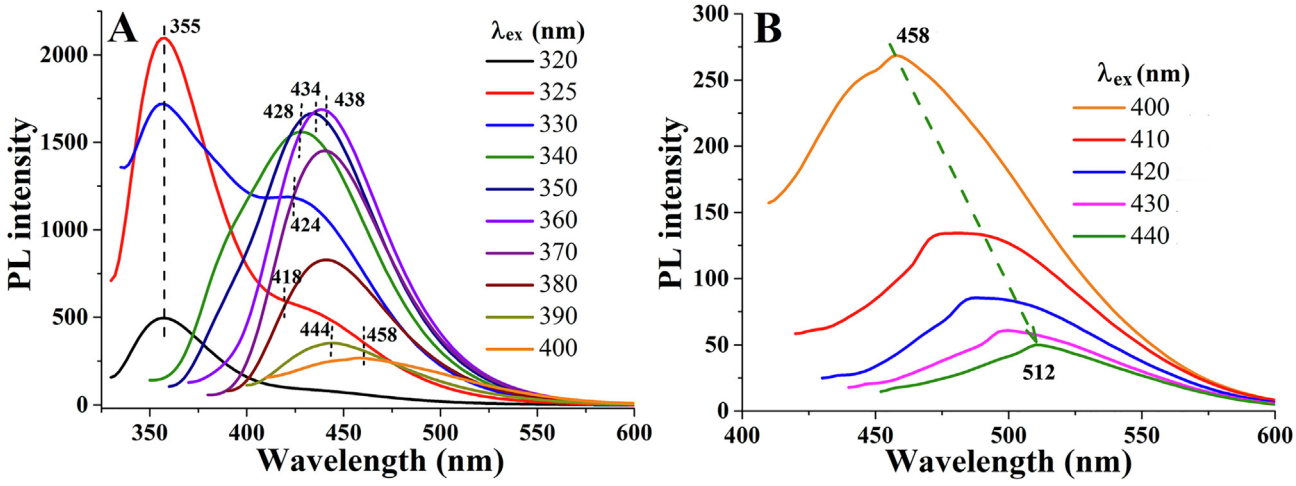

Fig. 3. Fluorescent spectra of TPU in DMSO solution (5 mg/mL) at different excitation: λ_{ex} from 320 to 400 nm (A) and from 400 to 440 nm (B).

[30,31]. TPU did not show any emission at 280 nm, and emitted at λ_{em} = 355 nm instead. Benzene ring was reportedly red-shifted through two different ways [30]: One is their π-π stacking in aggregates or crystals, which was clearly not happening in TPU solution; the other is electron delocalization in conjugated structure which is unlikely from TPU structure.

In fact, conjugation or sharing of electrons between heteroatoms and phenyl ring have been proposed for different molecules [30–34], in which at least one heteroatom was directly bonded to phenyl ring, including phenol, aniline and 4-(N,N′-dimethylamino)benzonitrile. It is suggested that, the electron donor substituents, such as OH and NH_2, contribute to increase electron density in π conjugation of a phenyl ring, and this is achieved by twisted intramolecular configuration of the substituent when it is out of the plane of the phenyl ring [32,33]. And the fluorescence behavior of these molecules is affected by the polarity of the solvent used. As to TPU, it has two urea units directly attached to phenyl ring through N atoms, of which the electrons are mostly in hybrid orbital of sp^2 [31], conjugation is believed to occur between the lone-pair electrons of N atom and the π electrons on the phenyl ring, reducing the energy required for their excitation and red-shifting therefore the fluorescent emission [35,36]. Seeing that each phenyl is substituted by two urea units, and their N atoms are separated by a carbonyl, it is therefore highly likely that the π electrons of the carbonyl are also conjugated, making the whole TPU chain like a conjugated one. This might be the reason for the emission at λ_{em} = 355 nm, largely red-shifted in comparison with that around 280 nm expected for a bare phenyl ring [30,31].

To support to this conclusion, four model compounds were synthesized (Fig. S2), and denoted as M1, M2, M3 and M4. Their structures were checked and confirmed by ^{1}H NMR (Fig. S4). All the four model molecules are consisted of phenyl ring(s) and urea unit(s) but connected in different ways (Fig. 4). From a view point of likelihood to conjugate for the phenyl ring, the similarity of these model molecules to TPU is summarized as follows: The phenyl ring of M1 is connected to two urea groups, a structure the closest to TPU; For M2, each of its phenyl rings has only one urea attached, which is connected to another methyl-substituted phenyl ring, the environment similarity of the phenyl ring to that of TPU is lessened compared to M1; For M3, the similarity of the chemical environment to TPU is further enlarged because one side of urea is replaced by a butyl; As to M4, the chemical environment for its phenyl ring is completely different from that in TPU, because of the insertion of ethylene spacer between phenyl rings and urea group, their possible conjugation, if any, must be disrupted. Instead, the chemical environment for its phenyl rings must be the most similar to that of benzene in comparison with M1 to M3. Each of the four compounds was dissolved in DMSO to have their solutions (0.01 mg/mL), and UV absorbance was measured for each, along with benzene and TPU (Fig. S5). From their absorbance bands (Table S3), it was seen that only one single absorbance band at 261 nm was present for benzene, attributed to its π-π* transition [37,38], while there were two bands for TPU at 256 and 300 nm, attributed respectively to, π-π* and n-π* transitions of its phenyl ring, owing to conjugation with N atoms and even the carbonyl double bond [35]. In comparison, all the four model compounds exhibited an absorbance band around 260 nm in accordance with that of benzene (261 nm). Besides this band, other bands at longer wavelength were also observed for all the model compounds: an absorbance at 300 nm (with a shoulder at 287 nm) for M1 and at 296 nm for M2, in accordance with the absorbance at 300 nm for M1. For M3, a number of shoulder bands were seen from 271 to 296 nm; and for M4, this band shifted to 270 nm, the most separated from that of TPU (300 nm), in accordance with the distinct difference in the chemical environment of its phenyl ring from that of TPU. These results indicate that the absorbance bands of the model compounds were more similar to those of TPU when the chemical environment in the molecules was closer to that in TPU.

Based on the results, under the same excitation (λ_{ex} = 300 nm) as for TPU solution to exhibit emission in UV region, emission behavior of the model molecules were tested in their DMSO solution at different concentrations, including M4 despite its very low absorbance as shown above (Fig. S5). Briefly, all the three compounds (M1, M2 & M3) were more emissive than M4 (Fig. S6). For M1, the maximal emission appeared at λ_{em} = 323 nm (Fig. S6A), and was unchanged with concentration; M3 exhibited practically the same emission behaviors, with its maximal emission equally at λ_{em} = 323 nm, unchanged with regard to its concentration. For both, their maximal emission intensities appeared at 1.0 mg/mL (Fig. S6). In contrast, M2 behaved slightly different in two ways (Fig. S6B): the maximal emission red-shifted to 352 nm, much closer to that of TPU, and the maximal intensity

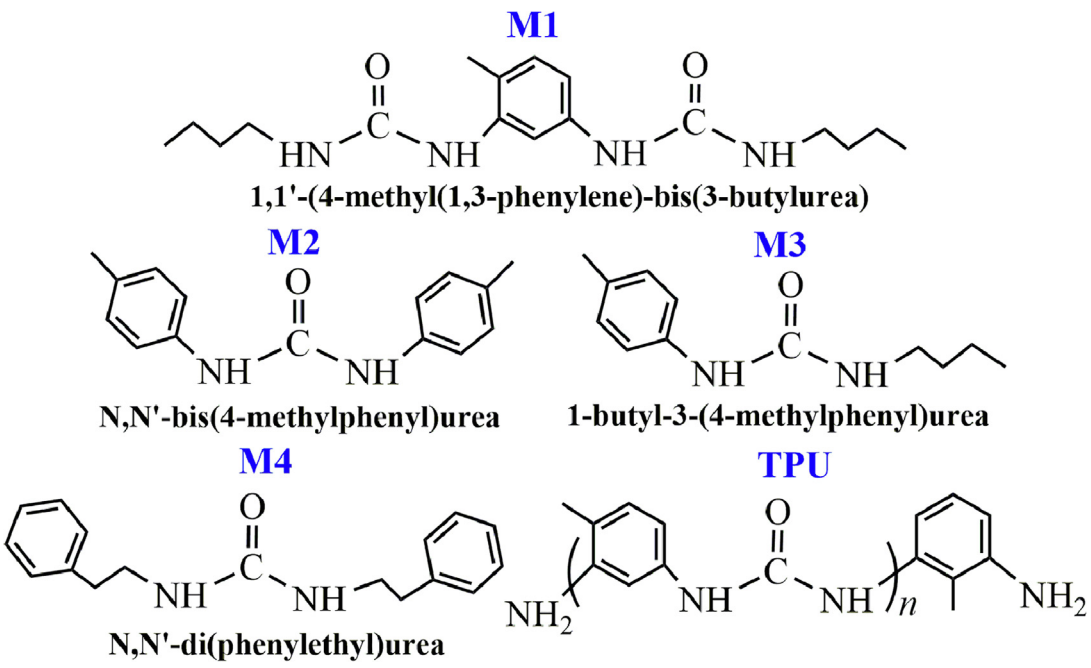

Fig. 4. Chemical structures of the four model compounds and TPU.

occurred at 2.0 mg/mL, instead of at 1.0 mg/mL in M1 and M3. This emission similarity of M2 to TPU might indicate the emission center was the urea unit rather than the phenyl. All these properties were very similar to TPU as shown above (Fig. 2A, B), except the maximal emission intensity (λ_{em} = 323 nm for M1, M3; λ_{em} = 352 nm for M2), which was different from TPU (λ_{em} = 355 nm). This may be a good support for the presence of extended conjugation of the phenyl ring to carbonyl through N atoms of its urea unit, making a more distinct red-shift for TPU emission.

In addition, M4 emission was also examined at different concentrations. A very weak emission was observed even under optimal conditions, the maximal intensity was about 1/10 of those observed for M1 and M3 (Fig. S6D). This was highly expected because, different from TPU and the other three model molecules, the phenyl rings in M4 were separated from its urea unit by an ethylene spacer, the conjugation of the phenyl ring with the urea unit was completely cut off. Through the comparisons of TPU structure, its absorbance and emission behaviors with those of the model compounds, it was concluded that, the emission of TPU in UV region (λ_{em} = 355 nm) was caused by its phenyl ring conjugated with the adjacent N atoms and the carbonyl groups of its urea units.

3.2.2. TPU emission in visible region

As shown in Fig. 3 and Table S2, under excitation of different wavelength ($\lambda_{ex} \geq$ 330 nm), TPU was highly emissive in visible region ($\lambda_{em} \geq$ 424 nm), with obvious EDE behavior. We suggest that this emission belonged most likely to the afore-mentioned CTE mechanism, i.e. owing to the formation of clusters upon aggregation of heteroatoms on the polymer chains [4–6,21]. In the clusters, the electron clouds of these so-called unconventional or intrinsically fluorescent groups are overlapped, offering therefore the molecules with extended conjugations (lowered energy gaps) and rigidified conformations. This type of emission and its intensity are usually dependent on the size of the cluster [5,6], leading to EDE behavior because the cluster size is concentration dependent. EDE has been well previously reported, mainly on carbon-based nanomaterials [39–44], commonly featured by their C atoms with hybrid orbital of sp3 or sp2, and chemical groups with O atoms [41,43]. Size effect has been the widely accepted theory for this behavior [41–43], i.e. the energy band gap is determined by the size and size distribution of a carbon nanomaterial, and emission is determined by this band gap. In contrast, EDE has been reported in a lessened extent for fluorescent polymers [21,23,45–50]. Among those reported, a great part has been focused on those without conventional chromophores [4–6,45–50], namely non-traditional intrinsic luminescent polymers [5] or intrinsically fluorescent [4]. For examples, EDE behavior was reported on poly(amino ester) and attributed to the cluster formation owing to the ester and tertiary amine groups, making n–π* electron transition possible from the tertiary amino to aggregated C = O [48]; Similar EDE was also reported on poly(maleic anhydride-alt-vinyl pyrrolidone), and was ascribed to the intra- and/or interchain interactions between N and O atoms as the result of the aggregation or clustering of the polymer chains [49]. Up to date, a huge number of studies have been reported on diverse polymers, which contain heteroatoms (N, O, S, P etc.) under the form of carbonyl, ester, hydroxyl, ether, amino, amide etc [20,21,27,42,45]. These polymers, of which the monomers are not fluorescent, do not contain conventional chromophores, and therefore do not emit at low concentration [20]; or, they contain in some cases conventional chromophores, such as phenyl group, and are not emissive or show weak emission in UV zone only [42,46,47]. However, they do show high emission in visible region at a higher concentration, and the emission is usually EDE featured. This type of emission behavior has been observed and widely studied. A variety of interpretations have been offered by different authors in different case studies. The most accepted and widely accepted mechanism is the CTE [20,21,45], proposed by Tang et al based on a study on pure oxygenic nonconjugated poly(maleic anhydride-alt-vinyl acetate) [20], they suggested that the formation of a heterodox cluster of carbonyl groups was the reason for the polymer to be emissive under UV excitation, and that the absorption and emission shifts to longer wavelength was due to the solvatochromism, i.e. the formation of polymer–solvent complexes due to the interaction of the polymer with electron-rich solvents. Under CTE mechanism, the photophysical behaviors of many polymers with neither conventional chromophores nor conjugated structures have been well interpreted [21,45,49–51].

Taking into accounts these analyses, the structure of TPU and its emission behavior described above (Figs. 2 & 3), it is strongly believed that the emission in the visible region ($\lambda_{em} \geq$ 424 nm under $\lambda_{ex} \geq$ 330 nm) must be owing to the cluster formation of TPU chains, rich of urea groups consisting of carbonyl, O and N atoms. At low concentration under excitation of long wavelength light ($\lambda_{ex} \geq$ 330 nm), TPU did not emit in the visible region because its chains were individually dissolved in DMSO and largely distanced each other. With increased concentration, the chains became much closer, clusters were formed through, probably, the hydrogen bonding of their O and N atoms with the H atoms of neighboring chains, well known for polyureas [26,29,52,53], making the interaction easier for the electrons on the carbonyl double bonds and on O and N atoms, promoting a delocalization for these electrons, along with those in the conjugated phenyl ring, and leading to the fluorescent emission in the visible region. Obviously, the number and size of the clusters were dependent on TPU concentration, so was the EDE observation for the fluorescent emission.

3.3. Tests of cluster formation

As described above, TPU emission in visible region was believed to be owing to cluster formation of TPU chains due to interaction of their functional groups. To support this conjecture, TPU solution in DMSO at different concentrations was prepared, and DLS test was conducted to explore the presence of the expected clusters [54]. The results revealed that clusters or aggregates were indeed occurring in TPU solution under certain circumstances. While DLS test did not provide any particles at concentration of 0.05 mg/mL or lower, particles or clusters of very small size (~0.8 nm) were effectively detected in TPU solution at concentration of 0.1 mg/mL, and this size was in regular increase with TPU concentration, as displayed in Fig. 5: the size of the clusters was increasing quite slowly at low TPU concentration, to 2.4 nm and 4.3 nm, respectively, at TPU concentration of 0.2 and 0.8 mg/mL; This increase in size (to 27 nm) was much sharper once TPU concentration increased to 1 mg/mL, and further to 83 nm with TPU concentration at 2 mg/mL. The size increase in the clusters became slower after the

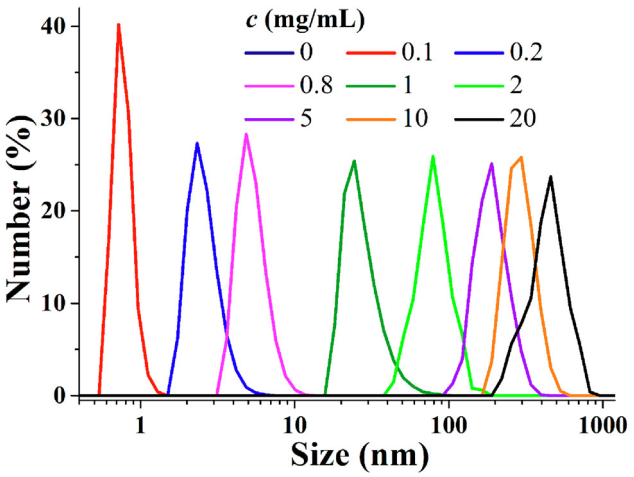

Fig. 5. Particles size detected by DLS in TPU solution at different concentrations.

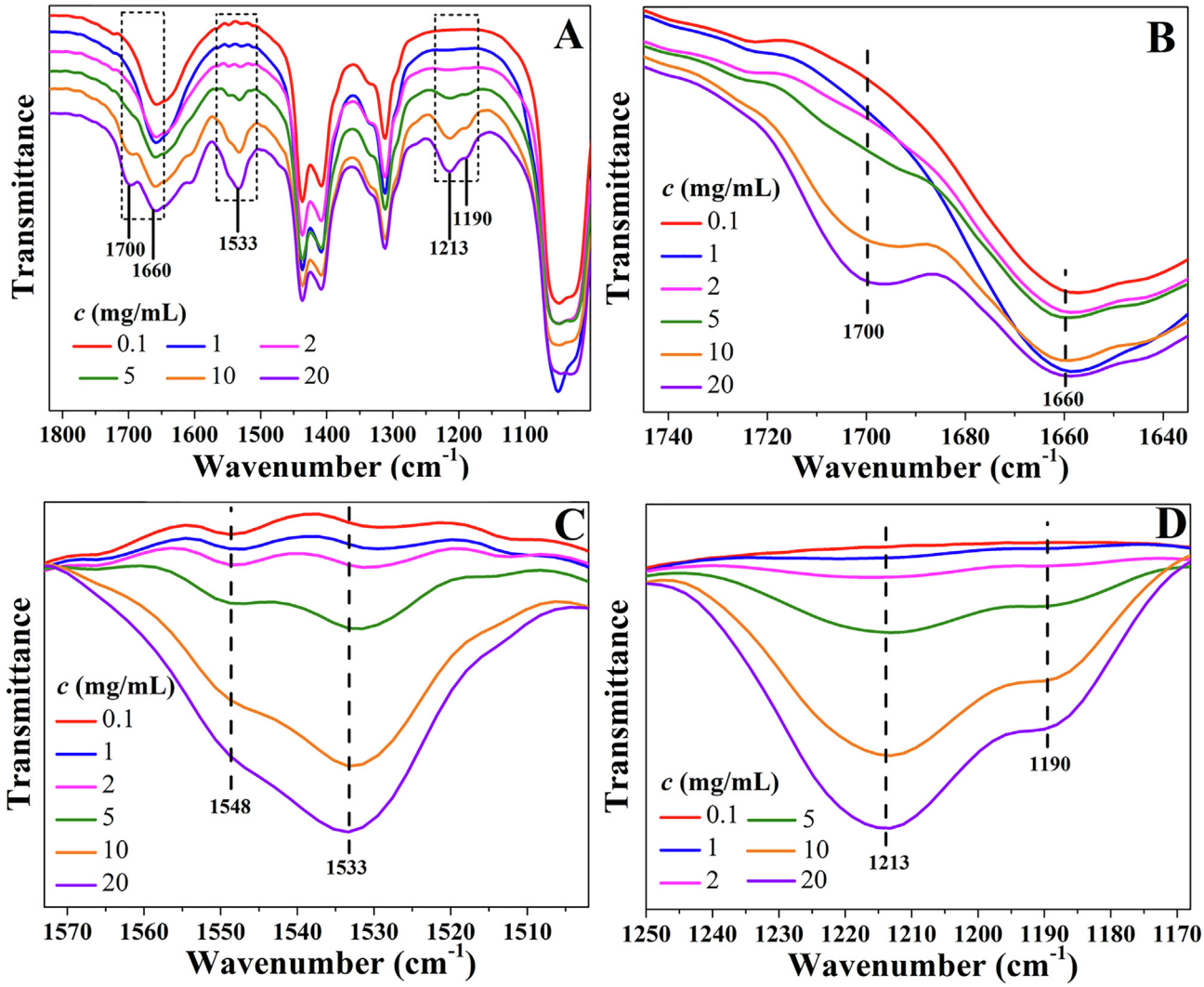

Fig. 6. FTIR spectra of TPU solutions in DMSO at different concentrations (A); Enlarged spectra of the absorbance zones from 1640 to 1740 cm^{-1} (B); from 1510 to 1570 cm^{-1} (C); from 1170 to 1250 cm^{-1} (D).

concentration reached 5 mg/mL (Fig. S7), and an average size of 403 nm was obtained at TPU concentration of 20 mg/mL. Comparing to the emission spectra of TPU solution at different concentrations (Fig. 2), it was found that the emission at 440 nm (under λ_{ex} = 350 nm) started to be significant at TPU concentration around 1 to 2 mg/mL, which was in good consistence with the detection of large-sized cluster of about 83 nm, suggesting strongly that this emission at 440 nm was owing to the cluster formation, in accordance with the CTE mechanism given in the section above.

It is easy to conceive that interactions between TPU chains, in particular the segments with electron rich groups, must be affected by the cluster formation, and reflected in their spectroscopic characterization such as FTIR [45,55–57]. Following the size detection by DLS, TPU solutions of different concentrations were subjected to FTIR analysis (Fig. 6). The absorbance of TPU carbonyl (C = O) appeared around 1660 cm^{-1}, slightly red-shifted owing to likely the presence of amides at its two sides [58–60]. However, a new absorbance band appeared at 1700 cm^{-1} with TPU concentration increased to 2.0 mg/mL (Fig. 6B), and it was significantly enhanced with increased concentration. This was indicating that TPU chains were presented under a new form, with higher electron density around their carbonyl groups. By cluster formation, it is assumed that the electrons on each group, including the carbonyls, the amide N atom and the phenyl rings, previously limited to each group, are shared among these groups in a cluster because of their conjugation and the clustering. The appearance of this absorbance at short wavelength (long wave number) at 1700 cm^{-1} seemed to indicate an increase in electron density around the carbonyls. As to the broad absorbance at 1525–1550 cm^{-1}, there were basically two absorbance bands like in polyurethane [45] and peptide [61] (Fig. 6C). The one around 1533 cm^{-1} is attributed to the bending vibration of N–H (amide II) in urea group and the other at 1548 cm^{-1} to the stretching vibration of the phenyl ring [62]. At low concentration (2.0 mg/mL), the two were of about equal intensity. However, with increased concentration in TPU, the one at 1548 cm^{-1} was attenuated relative to that at 1533 cm^{-1}, and the later was obviously enhancing, indicating a clustering with the amide as the center. In addition, the peak around 1533 cm^{-1} was the result of a slight blue-shifting with increased TPU concentration, from 1528 cm^{-1} at 2.0 mg/mL to 1533 cm^{-1} at 20 mg/mL, an indication of electron density increase over urea groups owing to the cluster formation. Another quite distinct change was also observed in the broad absorbance band from 1170 cm^{-1} to 1250 cm^{-1} (Fig. 6D), attributed to the stretching vibrations of amide III, i.e. the C-N bonds in the urea unit [61,62]. There was practically no absorbance at low concentration (0.1 mg/mL), and two absorbance bands started to appear at 2.0 mg/mL, indicating that, not only the carbonyl but also the adjacent C-N bond vibration was affected. It is to note that these changes in the absorbance bands became obvious only when TPU concentration attained 2.0 mg/mL, which

might be considered as the sign of the cluster formation, in agreement with the emission behavior seen above (Table S1), and at this concentration TPU became obviously emissive with discernable EDE behavior.

It is well known that, for a material under irradiation, the electrons on the out-layer of its atoms excite to a higher energy orbital by absorbing photons. Emission occurs when the excited electrons return back to their initial state by release of the absorbed energy through light radiation. UV absorbance is therefore often used to explore the mechanism of emission [23,63]. TPU solution in DMSO was subjected to UV absorbance. The results (Fig S5B) revealed that all the solutions, with concentration varied from 10^{-3} mg/mL to 20 mg/mL, had UV absorbance bands, and that the maximal absorbance wavelength red-shifted with increased concentration. At concentration of 10^{-3} mg/mL, only one sharp absorbance at 256 nm was present, indicating likely that TPU chains were assumingly well dissolved; with concentration increased to 10^{-2} mg/mL, a new absorbance appeared around 300 nm, making TPU emissive at 355 nm as shown in Fig. 2A. It is to note that this new absorbance around 300 nm was boosted quite fast with increased TPU concentration, leading to enhanced emission as seen in Fig. 2A, owing to the conjugation between the π electrons of the carbonyl and the phenyl ring through N atom in between, as discussed in section 3.2. It is particularly interesting that, starting from the concentration at 2 mg/mL, another new absorbance at 350 nm was detected, suggesting that a new type of matter was created, i.e. the formation of TPU clusters. It was exactly this cluster formation, which led to the new and excitation dependent emission at around 440 nm, shown in Fig. 2C and Fig. 3A. All these results are in good agreement, and give substantial support to the CTE mechanism elaborated in section 3.2.2 based on cluster formation.

As supplementary information, it is to point out that polyurea is insoluble in common organic solvents, such as hexane, toluene, THF, acetone, pyridine and acetonitrile [64]. Among a dozen of solvents tested, the highest TPU concentration one can make is about 3 mg/mL in acetic acid and in m-cresol, which renders the comparison of the solvent effect on TPU emission difficult. TPU is only soluble in DMSO, N,N-dimethyl formamide (DMF) and N-methyl-2-pyrrolidone (NMP), up to concentration at 20 mg/mL or higher. Fluorescent emission was tested in DMF and NMP at different TPU concentrations (0.05, 1.0 and 5.0 mg/mL), which showed exactly the same emission profile as those in DMSO (Fig. 3). The emission spectra of TPU at 5.0 mg/mL are given as an exemplar (Fig. S8). These results indicate that no discernable solvent effect was observed. This insensitivity of emission versus the tested solvents suggests the negligible solvent effect on the cluster structure, i.e. weak interaction between solvent and TPU chains, which is different from hyperbranched polysiloxane, where obvious changes of the emission intensity was observed in different solvents [65].

3.4. Quenching effect and application trials

To see the possibility for TPU as a sensor to detect metal ions, its emission was evaluated in the presence of a number of metal ions, each at concentration of 0.3 mM. Under UV lamp (λ_{ex} = 365 nm, Fig. S9), the emission, in the presence of Ag^+, Ni^{2+}, Ca^{2+}, Pb^{2+}, Cd^{2+} and Cu^{2+}, was practically the same as that in the pure solution of TPU showed in Fig. 1, and in the presence of Cu^+ and Fe^{2+}, the emission was slightly attenuated. In contrast, an obvious quenching effect was well seen in the presence of the ions Fe^{3+} under excitation of λ_{ex} = 350 nm, in comparison with the rest of the tested ions (Fig. 7A). And the emission practically disappeared when Fe^{3+} attained 0.54 mM (Fig. 7B). The co-presence of these tested ions at the same concentration (0.54 mM) as Fe^{3+} showed no disturbance on its quenching effect. The competitive ions appeared to behave as in the cases when they were individually present, with the emission slightly changed as seen in Fig. 7A. And the emission was practically turned off once Fe^{3+} was added along with the competitive ions, indicating high selectivity of Fe^{3+} quenching towards TPU emission (Fig. S10).

The quenching effect of Fe^{3+} has been often studied for different fluorescent materials [65–69]. Different mechanisms have been proposed for the selectivity of Fe^{3+}. Its larger charge/radius ratio is believed to be one possibility [65,69], which renders it with the strongest electron-withdrawing ability among all the ions tested. Another widely accepted mechanism is its paramagnetic nature, with its five d orbits half-filled under electronic structure of 3d5-4 s0. Fe^{3+} is also featured by its outstanding standard electrode potentials [66–68], higher than all the other metal ions examined but Ag^+ (Table S4). However, given the atomic numbers of Fe and Ag and their charges (3 to 1), Fe^{3+} has the highest charge density among all the metal ions used. All these combined, it is obvious that Fe^{3+} has the strongest electron-withdrawing ability among commonly seen metal ions, which makes it a common quencher via different quenching mechanisms [70].

The detection limit (DL) of Fe^{3+} was determined using a reported method [71], which gives: DL = k × σ/S, where σ is the standard deviation of the blank samples from at least 20 measures (σ = 0.218 in this work); S is analytical sensitivity, i.e. the slope of the measure signal (the emission intensity) versus the concentration of Fe^{3+} (the absolute value is used for negative slope); and k, a numerical factor chosen in accordance with desired confidence level. k < 3 should not be used for DL calculations, and use of k = 3 is suggested to allows a confidence level of 99.9%. In accordance, the emission intensity of TPU in DMSO (10 mg/mL) was recorded as a function of Fe^{3+} concentration (mM), and the results given in Fig. 8. It is seen that the emission intensity was linearly decreasing with increasing [Fe^{3+}] in the concentration range of 0–0.15 mM (Fig. 8A). The linearity curve in Fig. 8B gave a slope of −10558 with a correlation coefficient of 0.992. A value of 6.19×10^{-8} M for DL was thus obtained. In comparison to reported studies on Fe^{3+} detection systems, where DL values varied from 1.0×10^{-6} to 2.1×10^{-8} M were obtained (Table S5), DL of this work is similar to or better than all the reported data. Taking into account of the easy preparation, it is quite obvious that TPU is a material of choice for Fe^{3+} detection in view of its easy fabrication and low DL.

Based on the quenching effect of Fe^{3+} on TPU emission, a paper strip was dipped into a solution of TPU in DMSO at 30 mg/mL, TPU remained on the surface of the paper after drying up. Under UV lamp (365 nm), this paper strip showed strong blue color as shown by Fig. 9A. By drawing a letter “K” using a pipette filled with Fe^{3+} aqueous solution (0.03 mM), that letter turned non-emissive because of the quenching effect (Fig. 9B). This can be used for easy Fe^{3+} detection in aqueous system.

Based on the quenching of TPU by Fe^{3+}, a security paper for data encryption can be made from an ordinary (no fluorescent) paper by dipping it in TPU solution. This TPU coated paper was blue luminescent under UV lamp (365 nm, Fig. 10A). By writing “COVID-19” on the paper with an aqueous solution of disodium salt of ethylene diamine tetraacetic acid (Na_2EDTA, 10 mg/mL) as the ink, no any changed was observed by naked eye under daylight or UV irradiation (Fig. 10B), which meant that the information was successfully encrypted. However, “COVID-19” was clearly seen under UV lamp (Fig. 10C) by brushing the security paper with an aqueous solution of $FeCl_3$ (1.0 mM). This is because Fe^{3+} ions interacted in priority with Na_2EDTA against TPU, protecting TPU fluorescence from quenching by Fe^{3+} ions. $FeCl_3$ is used here as the key to decode the encrypted information on the security paper. Therefore, TPU can be used as a tool to fabricate security paper for data encryption.

In contrast with Fe^{3+} ions, Fe^{2+} ions have no quenching effect on TPU emission as shown in Fig. 7A. Based on this point, a fluorescent paper strip was made by dipping it into a solution of TPU with the presence of Fe^{2+} ions, which, under UV irradiation, showed the same bright blue color as that in Fig. 10A (the paper dipped in TPU without the presence of Fe^{2+} ions). By writing any letters on this fluorescent strip using an aqueous solution of an oxidant (such as H_2O_2 and *tert*-butyl hydroperoxide) as the ink, these letters were well readable under

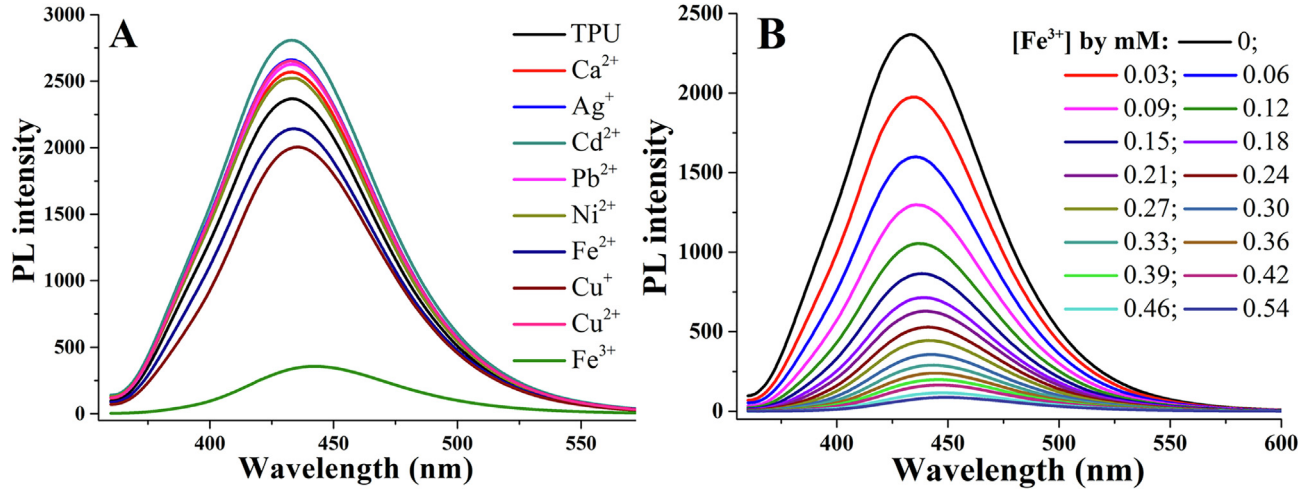

Fig. 7. Emission spectra of TPU solution (10 mg/mL) in DMSO in the presence of different metal ions (0.3 mM) under excitation of λ_{ex} = 350 nm (A), and those in the presence of Fe^{3+} solution of different concentrations under excitation of λ_{ex} = 350 nm (B).

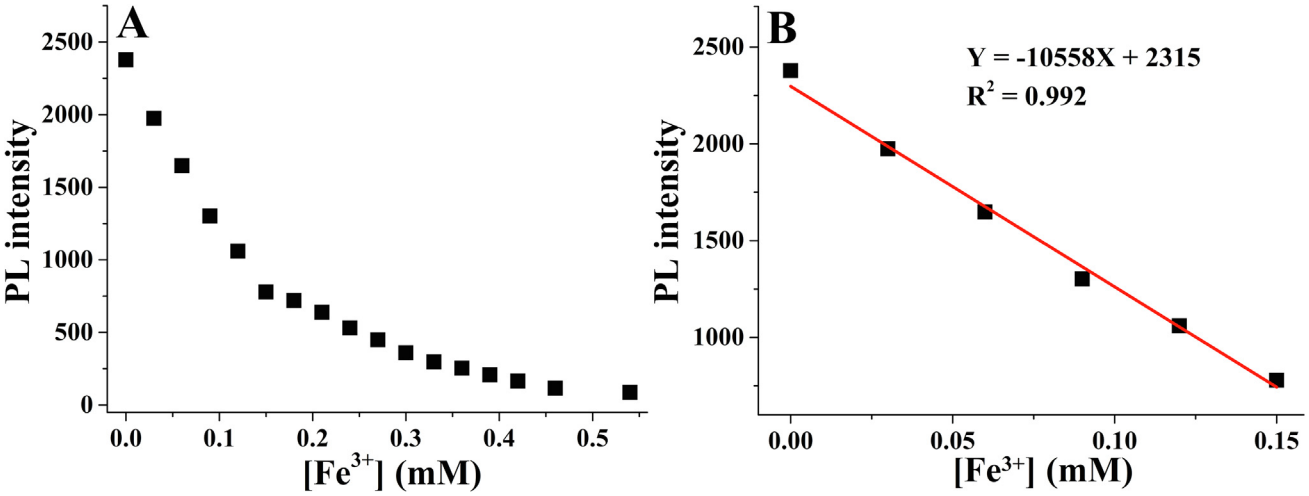

Fig. 8. Emission intensity of TPU solution (10 mg/mL) as function of Fe^{3+} concentration (mM) under λ_{ex} = 350 nm (A), and linear relationship of the emission intensity versus Fe^{3+} concentration from 0 to 0.15 mM (B).

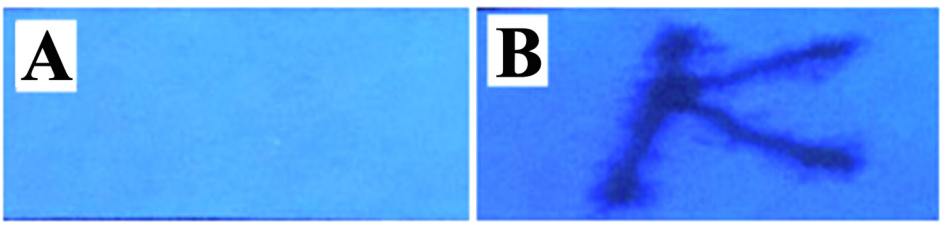

Fig. 9. Photo of a paper strip dipped in DMSO solution of TPU (30 mg/mL) under UV lamp (A), the same paper after drawing letter K using aqueous solution of Fe^{3+} ions (0.03 mM, B).

UV light because the paper covered by these letters became no fluorescent owing to Fe^{3+} formation from Fe^{2+} oxidation. This change in blue fluorescence was easily observable by naked-eyes with H_2O_2 concentration at 0.04 mM (Fig. S11). This is particularly interesting in biological detection of H_2O_2 in human body, because H_2O_2 is produced in metabolism process, and known as a precursor molecule of a number of reactive oxygen species, commonly known to cause oxidative damage on proteins and nucleic acids and to be correlated to cancer and Alzheimer's diseases [72].

4. Conclusions

Polyurea, TPU, was synthesized through a very easy protocol of precipitation polymerization of TDI in a binary solvent of water–acetone, and was emissive as powder and in its DMSO solution. In solution, TPU emission was covering a broad span from UV to visible region of up to 500 nm under different excitation. Under short wavelength excitation ($\lambda_{ex} \leq$ 320 nm), the emission started from concentration of as low as 10^{-5} mg/mL, passed a maximum at 355 nm, and faded off at higher concentration. The concentrations, where the emission started to appear, to maximize and to disappear, were closely dependent on the excitation. Under long wavelength excitation ($\lambda_{ex} \geq$ 350 nm), the emission at 355 nm disappeared, and a new emission appeared at about λ_{em} = 440 nm, which is featured by constant increase in intensity with TPU concentration and constant red-shifting under excitation with extended wavelength. Based on the results, it was proposed that the emission in UV region (λ_{em} = 355 nm) was ascribed to the chemical structure itself owing to an eventual

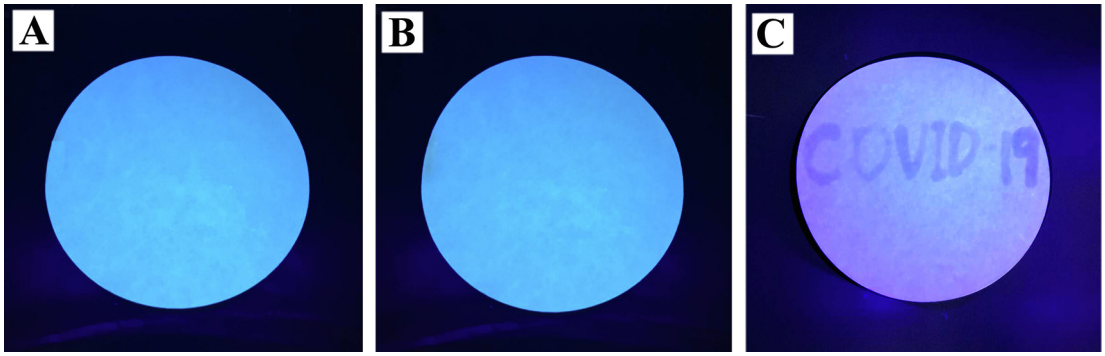

Fig. 10. Under UV lamp, photo of a paper strip dipped in DMSO solution of TPU (30 mg/mL) (A), after writing "COVID-19" using aqueous solution of Na_2EDTA (B), and the same paper strip brushed with aqueous solution of $FeCl_3$ (1.0 mM, C).

conjugation between the phenyl ring and the urea carbonyl through n-π* transition of the N atoms in between, which was supported by emission behaviors of four organic urea model compounds synthesized for this study. As to the strongly excitation dependent emission appeared at about λ_{em} = 440 nm under $\lambda_{ex} \geq$ 350 nm, it was attributed to the cluster formation of the TPU molecules, supported by DLS test for the presence of cluster particles, FTIR absorbance changes and UV absorbance at TPU concentration where this emission started to appear. By screening a number of metal ions, Fe^{3+} was shown to have an obvious quenching effect on TPU emission. Simple paper strips were fabricated by coating TPU on their surface, followed by different treatments by aqueous solutions of Fe^{3+}, Fe^{2+} or Na_2EDTA. These sensor paper strips were used for detections of Fe^{3+} and H_2O_2 in aqueous systems, and for data encryption.

Declaration of Competing Interest

The authors declare that they have no known competing financial interests or personal relationships that could have appeared to influence the work reported in this paper.

Acknowledgments

This research is financially supported by National Natural Science Foundation of China (Nos. 21274054, 21304038, 51473066), Natural Science Foundation of Shandong Province (Nos. ZR2018BB049, ZR2018MB021, ZR2019MB031), and by Science & Technology Development Plan (2017GGX202009) of Shandong Province, China.

Appendix A. Supplementary data

Supplementary data to this article can be found online at https://doi.org/10.1016/j.cej.2020.125867.

References

[1] C.D. Geddes, Reviews in Fluorescence 2017, Springer Nature Switzerland AG, Switzerland, 2018, https://doi.org/10.1007/978-3-030-01569-5.
[2] Z. Li, J.R. Askim, K.S. Suslick, The optoelectronic nose: Colorimetric and fluorometric sensor arrays, Chem. Rev. 119 (2019) 231–292, https://doi.org/10.1021/acs.chemrev.8b00226.
[3] E. Asadian, M. Ghalkhani, S. Shahrokhian, Electrochemical sensing based on carbon nanoparticles: A review, Sens. Actuators, B 293 (2019) 183–209, https://doi.org/10.1016/j.snb.2019.04.075.
[4] M.N. Liu, W.G. Chen, H.J. Liu, Y. Chen, Facile synthesis of intrinsically photoluminescent hyperbranched polyethylenimine and its specific detection for copper ion, Polymer 172 (2019) 110–116, https://doi.org/10.1016/j.polymer.2019.03.069.
[5] D.A. Tomalia, B. Klajnert-Maculewicz, K.A.M. Johnson, H.F. Brinkman, A. Janaszewska, D.M. Hedstrand, Non-traditional intrinsic luminescence: inexplicable blue fluorescence observed for dendrimers, macromolecules and small molecular structures lacking traditional/conventional luminophores, Prog. Polym. Sci. 90 (2019) 35–117, https://doi.org/10.1016/j.progpolymsci.2018.09.004.
[6] H. Zhang, Z. Zhao, P.R. McGonigal, R. Ye, S. Liu, J.W.Y. Lam, R.T.K. Kwok, W.Z. Yuan, J. Xie, A.L. Rogach, B.Z. Tang, Clusterization-triggered emission: uncommon luminescence from common materials, Mater. Today 32 (2020) 275–292, https://doi.org/10.1016/j.mattod.2019.08.010.
[7] Y. Guan, T. Sun, J. Ding, Z. Xie, Robust organic nanoparticles for noninvasive long-term fluorescence imaging, J. Mater. Chem. B 7 (2019) 6879–6889, https://doi.org/10.1039/c9tb01905g.
[8] K. Deng, X. Zhao, F. Liu, J. Peng, C. Meng, Y. Huang, L. Ma, C. Chang, H. Wei, Synthesis of thermosensitive conjugated triblock copolymers by sequential click couplings for drug delivery and cell imaging, ACS Biomater. Sci. Eng. 5 (2019) 3419–3428, https://doi.org/10.1021/acsbiomaterials.9b00664.
[9] I. Lee, S. Kim, S.N. Kim, Y. Jang, J. Jang, Highly fluorescent amidine/Schiff base dual-modified polyacrylonitrile nanoparticles for selective and sensitive detection of copper ions in living cells, ACS Appl. Mater. Interfaces 6 (2014) 17151–17156, https://doi.org/10.1021/am504824n.
[10] O.S. Wolfbeis, An overview of nanoparticles commonly used in fluorescent bioimaging, Chem. Soc. Rev. 44 (2015) 4743–4768, https://doi.org/10.1039/c4cs00392f.
[11] M. Storf, A. Parbel, M. Meyer, B. Strohmann, H. Scheer, Chromophore attachment to biliproteins: Specificity of PecE/PecF, a lyase-isomerase for the photoactive 3^1-Cys-α84-phycoviolobilin chromophore of phycoerythrocyanin, Biochemistry 40 (2001) 12444–12456, https://doi.org/10.1021/bi010776s.
[12] Z. Ning, H. Tian, Triarylamine: a promising core unit for efficient photovoltaic materials, Chem. Commun. (2009) 5483–5495, https://doi.org/10.1039/b908802d.
[13] T. Zhang, F. Wang, M. Li, J. Liu, J. Miao, B. Zhao, A simple pyrazoline-based fluorescent probe for Zn^{2+} in aqueous solution and imaging in living neuron cells, Sens. Actuators, B 186 (2013) 755–760, https://doi.org/10.1016/j.snb.2013.06.085.
[14] P.D. Barata, A.I. Costa, J.V. Prata, Calix[4]arene–carbazole-containing polymers: Synthesis and properties, React. Funct. Polym. 72 (2012) 627–634, https://doi.org/10.1016/j.reactfunctpolym.2012.06.006.
[15] T. Beltrani, M. Bösch, R. Centore, S. Concilio, P. Günter, A. Sirigu, Synthesis and electrooptic properties of side-chain methacrylate polymers containing a new azophenylbenzoxazole chromophore, J. Polym. Sci. A: Polym. Chem. 39 (2001) 1162–1168, https://doi.org/10.1002/pola.1093.
[16] C. Cojocariua, P. Rochon, Synthesis and optical storage properties of a novel polymethacrylate with benzothiazole azo chromophore in the side chain, J. Mater. Chem. 14 (2004) 2909–2916, https://doi.org/10.1039/B405711B.
[17] R. Karim, R.K. Sheikh, R. Yahya, N.M. Salleh, A.D. Azzahari, A. Hassan, N.M. Sarih, Thermal, optical and electrochemical study of side chain liquid crystalline polymers bearing azo-benzothiazole chromophore in the mesogen, J. Polym. Res. 20 (2013) 259, https://doi.org/10.1007/s10965-013-0259-5.
[18] D. Wang, T. Imae, Fluorescence emission from dendrimers and its pH dependence, J. Am. Chem. Soc. 126 (2004) 13204–13205, https://doi.org/10.1021/ja0454992.
[19] W.I. Lee, Y. Bae, A.J. Bard, Strong blue photoluminescence and ECL from OH-terminated PAMAM dendrimers in the absence of gold nanoparticles, J. Am. Chem. Soc. 126 (2004) 8358–8359, https://doi.org/10.1021/ja0475914.
[20] E. Zhao, J.W.Y. Lam, L. Meng, Y. Hong, H. Deng, G. Bai, X. Huang, J. Hao, B.Z. Tang, Poly [(maleic anhydride)-*alt*-(vinyl acetate)]: A pure oxygenic non-conjugated macromolecule with strong light emission and solvatochromic effect, Macromolecules 48 (2015) 64–71, https://doi.org/10.1021/ma502160w.
[21] W.Z. Yuan, Y. Zhang, Nonconventional macromolecular luminogens with aggregation-induced emission characteristics, J. Polym. Sci., Part A: Polym. Chem. 55 (2017) 560–574, https://doi.org/10.1002/pola.28420.
[22] J. Luo, Z. Xie, J.W.Y. Lam, L. Cheng, H. Chen, C. Qiu, H.S. Kwok, X. Zhan, Y. Liu, D. Zhu, B.Z. Tang, Aggregation-induced emission of 1-methyl-1,2,3,4,5-pentaphenylsilole, Chem. Commum. (2001) 1740–1741, https://doi.org/10.1039/b105159h.
[23] J. Mei, Y. Hong, J.W.Y. Lam, A. Qin, Y. Tang, B.Z. Tang, Aggregation-induced emission: The whole is more brilliant than the parts, Adv. Mater. 26 (2014) 5429–5479, https://doi.org/10.1002/adma.201401356.
[24] H. Han, Y. Zhou, S. Li, Y. Wang, X.Z. Kong, Immobilization of lipase from pseudomonas fluorescens on porous polyurea and its application in kinetic resolution of racemic 1-phenylethanol, ACS Appl. Mater. Interfaces 8 (2016) 25714–25724,

https://doi.org/10.1021/acsami.6b07979.
[25] Y. Wei, X. Jiang, S. Li, X.Z. Kong, Catalysis of isocyanate reaction with water by DMF and its use for fast preparation of uniform polyurea microspheres through precipitation polymerization, Eur. Polym. J. 115 (2019) 384–390, https://doi.org/10.1016/j.eurpolymj.2019.03.054.
[26] X. Zhang, S. Li, X. Zhu, X. Jiang, X.Z. Kong, Easy preparation of porous polyurea through copolymerization of toluene diisocyanate with ethylenediamine and its use as absorbent for copper ions, React. Funct. Polym. 133 (2018) 143–152, https://doi.org/10.1016/j.reactfunctpolym.2018.10.010.
[27] R.B. Restani, P.I. Morgado, M.P. Ribeiro, I.J. Correia, A. Aguiar-Ricardo, V.D.B. Bonifacio, Biocompatible polyurea dendrimers with pH-dependent fluorescence, Angew. Chem. Int. Ed. 51 (2012) 5162–5165, https://doi.org/10.1002/anie.201200362.
[28] X. Jiang, M.S. Bashir, F. Zhang, X.Z. Kong, Formation and shape transition of porous polyurea of exotic forms through interfacial polymerization of toluene diisocyanate in aqueous solution of ethylenediamine and their characterization, Eur. Polym. J. 109 (2018) 93–100, https://doi.org/10.1016/j.eurpolymj.2018.09.002.
[29] H. Han, S. Li, X. Zhu, X. Jiang, X.Z. Kong, One step preparation of porous polyurea by reaction of toluene diisocyanate with water and its characterization, RSC Adv. 4 (2014) 33520–33529, https://doi.org/10.1039/C4RA06383J.
[30] J.J. Yan, Z.K. Wang, X.S. Lin, C.Y. Hong, H.Y. Liang, C.Y. Pan, Y.Z. You, Polymerizing nonfluorescent monomers without incorporating any fluorescent agent produces strong fluorescent polymers, Adv. Mater. 24 (2012) 5617–5624, https://doi.org/10.1002/adma.201202201.
[31] B. Wang, H. Xi, Y. Zhou, X. Chen, X. Fu, Effect of different substituent on three dimensional fluorescence properties of BTEX, Spectrosc. Spect. Anal. 37 (2017) 3763–3770, https://doi.org/10.3964/j.issn.1000-0593(2017)12-3763-08.
[32] R.J. Visser, C.A.G.O. Varma, Source of anomalous fluorescence from solutions of 4-N,N-dimethylaminobenzonitrilein polar solvents, J. Chem. Soc., Faraday Trans. II 76 (1980) 453–471, https://doi.org/10.1039/F29807600453.
[33] A. Broo, M.C. Zerner, Calculations of the absorption and emission spectra of p-N, N-dimethylaminobenzonitrile and analogues in solution, Thero. Chim. Acta 90 (1995) 383–395, https://doi.org/10.1007/BF01113543.
[34] I.F. Galván, M.E. Martín, M.A. Aguilar, Theoretical study of the dual fluorescence of 4-(N, N-dimethylamino)benzonitrile in solution, J. Chem. Theory Comput. 6 (2010) 2445–2454, https://doi.org/10.1021/ct9006713.
[35] N. Jiang, G.F. Li, B.H. Zhang, D.X. Zhu, Z.M. Su, M.R. Bryce, Aggregation-induced long-lived phosphorescence in nonconjugated polyurethane derivatives at 77 K, Macromolecules 51 (2018) 4178–4184, https://doi.org/10.1021/acs.macromol.8b00715.
[36] Q. Wan, M. Liu, L. Mao, R. Jiang, D. Xu, H. Huang, Y. Dai, F. Deng, X. Zhang, Y. Wei, Preparation of PEGylated polymeric nanoprobes with aggregation-induced emission feature through the combination of chain transfer free radical polymerization and multicomponent reaction: Self-assembly, characterization and biological imaging applications, Mater. Sci. Eng., C 72 (2017) 352–358, https://doi.org/10.1016/j.msec.2016.11.058.
[37] C.Z. Zhu, R.X. Zhang, G.M. Zheng, B. Ouyang, Q.X. Zhao, H.Q. Hou, Reaction mechanism of aqueous benzene with hydrogen peroxide by transient absorbance spectra, Acta Phys. -Chim. Sin. 20 (2004) 1112–1117, https://doi.org/10.3866/PKU.WHXB20040911.
[38] S. Camou, A. Shimizu, T. Horiuchi, T. Haga, Selective aqueous benzene detection at ppb level with portable sensor based on pervaporation extraction and UV-spectroscopy, Procedia Chem. 1 (2009) 1495–1498, https://doi.org/10.1016/j.proche.2009.07.373.
[39] D. Pan, J. Zhang, Z. Li, M. Wu, Hydrothermal route for cutting graphene sheets into blue-luminiscent graphene quantum dots, Adv. Mater. 22 (2010) 734–738, https://doi.org/10.1002/adma.200902825.
[40] V.N. Mochalin, Y. Gogotsi, Wet chemistry route to hydrophobic blue fluorescent nanodiamond, J. Am. Chem. Soc. 131 (2009) 4594–4595, https://doi.org/10.1021/ja9004514.
[41] Z. Gan, S. Xiong, X. Wu, T. Xu, X. Zhu, X. Gan, J. Guo, J. Shen, L. Sun, P.K. Chu, Mechanism of photoluminescence from chemically derived graphene oxide: Role of chemical reduction, Adv. Opt. Mater. 1 (2013) 926–932, https://doi.org/10.1002/adom.201300368.
[42] Z. Gan, X. Wu, Y. Hao, The mechanism of blue photoluminescence from carbon nanodots, CrystEngComm 16 (2014) 4981–4986, https://doi.org/10.1039/c4ce00200h.
[43] S. Zhu, Q. Meng, L. Wang, J. Zhang, Y. Song, H. Jin, K. Zhang, H. Sun, H. Wang, B. Yang, Highly photoluminescent carbon dots for multicolor patterning, sensors, and bioimaging, Angew. Chem. 125 (2013) 4045–4049, https://doi.org/10.1002/ange.201300519.
[44] Y. Song, S. Zhu, B. Yang, Bioimaging based on fluorescent carbon dots, RSC Adv. 4 (2014) 27184–27200, https://doi.org/10.1039/c3ra47994c.
[45] X. Chen, X. Liu, J. Lei, L. Xu, Z. Zhao, F. Kausar, X. Xie, X. Zhu, Y. Zhang, W.Z. Yuan, Synthesis, clustering-triggered emission, explosive detection and cell imaging of nonaromatic polyurethanes, Mol. Syst. Des. Eng. 3 (2018) 364–375, https://doi.org/10.1039/c7me00118e.
[46] W. Liu, X. Tian, J. Zheng, P. Cui, Excitation dependence of the photoluminescence of poly(ethylene terephthalate), Acta Polym. Sin. 4 (2005) 637–640, https://doi.org/10.1016/j.carbpol.2005.04.003.
[47] H. Itagaki, Y. Inagaki, N. Kobayashi, Microenvironments in poly(ethylene terephthalate) film revealed by means of fluorescence measurements, Polymer 37 (1996) 3553–3558, https://doi.org/10.1016/0032-3861(96)00208-X.
[48] L. Yuan, H. Yan, L. Bai, T. Bai, Y. Zhao, L. Wang, Y. Feng, Unprecedented multicolor photoluminescence from hyperbranched poly(amino ester)s, Macromol. Rapid Commun. 40 (2018) 1800658, https://doi.org/10.1002/marc.201800658.
[49] C. Shang, N. Wei, H. Zhuo, Y. Shao, Q. Zhang, Z. Zhang, H. Wang, Highly emissive poly(maleic anhydride-*alt*-vinyl pyrrolidone) with molecular weight-dependent and excitation-dependent fluorescence, J. Mater. Chem. C 5 (2017) 8082–8090, https://doi.org/10.1039/C7TC02381B.
[50] X. Miao, T. Liu, C. Zhang, Xi Geng, Y. Meng, X. Li, Fluorescent aliphatic hyperbranched polyether: chromophore-free and without any N and P atoms, Phys. Chem. Chem. Phys. 18 (2016) 4295–4299, https://doi.org/10.1039/C5CP07134H.
[51] H. Lu, L. Feng, S. Li, J. Zhang, H. Lu, S. Feng, Unexpected strong blue photoluminescence produced from the aggregation of unconventional chromophores in novel siloxane-poly(amidoamine) dendrimers, Macromolecules 48 (2015) 476–482, https://doi.org/10.1021/ma502352x.
[52] J. Xu, H. Han, L. Zhang, X. Zhu, X. Jiang, X.Z. Kong, Preparation of highly uniform and crosslinked polyurea microspheres through precipitation copolymerization and their property and structure characterization, RSC Adv. 4 (2014) 32134–32141, https://doi.org/10.1039/c4ra04206a.
[53] R.T. Shafranek, J.D. Leger, S. Zhang, M. Khalil, X. Gu, A. Nelson, Sticky ends in a self-assembling ABA triblock copolymer: the role of ureas in stimuli-responsive hydrogels, Mol. Syst. Des. Eng. 4 (2019) 91–102, https://doi.org/10.1039/c8me00063h.
[54] Q. Wang, B. Li, H. Cao, X. Jiang, X.Z. Kong, Aliphatic amide salt, a new type of luminogen: Characterization, emission and biological applications, Chem. Eng. J. 388 (2020) 124182, , https://doi.org/10.1016/j.cej.2020.124182.
[55] B. Zhang, H. Tang, P. Wu, In depth analysis on the unusual multistep aggregation process of oligo(ethylene glycol) methacrylate-based polymers in water, Macromolecules 47 (2014) 4728–4737, https://doi.org/10.1021/ma500774g.
[56] S. Sun, P. Wu, Role of water/methanol clustering dynamics on thermosensitivity of poly(n-isopropylacrylamide) from spectral and calorimetric insights, Macromolecules 43 (2010) 9501–9510, https://doi.org/10.1021/ma1016693.
[57] A. Chaari, C. Fahy, A. Chevillot-Biraud, M. Rholam, Investigating the effects of different natural molecules on the structure and oligomerization propensity of hen egg-white lysozyme, Int. J. Biol. Macromol. 134 (2019) 189–201, https://doi.org/10.1016/j.ijbiomac.2019.05.048.
[58] X. Zhang, X. Jiang, X. Zhu, X.Z. Kong, Effective enhancement of Cu ions adsorption on porous polyurea adsorbent by carboxylic modification of its terminal amine groups, React. Funct. Polym. 147 (2020) 104450, , https://doi.org/10.1016/j.reactfunctpolym.2019.104450.
[59] A. Pangon, G.P. Dillon, J. Runt, Influence of mixed soft segments on microphase separation of polyurea elastomers, Polymer 55 (2014) 1837–1844, https://doi.org/10.1016/j.polymer.2014.02.009.
[60] J.T. Garrett, R. Xu, J. Cho, J. Runt, Phase separation of diamine chain-extended poly(urethane) copolymers: FTIR spectroscopy and phase transitions, Polymer 44 (2003) 2711–2719, https://doi.org/10.1016/S0032-3861(03)00165-4.
[61] R. Wu, T.B. McMahon, Protonation sites and conformations of peptides of glycine ($(Gly_{1-5}H^+)$) by IRMPD spectroscopy, J. Phys.Chem. B 113 (2009) 8767–8775, https://doi.org/10.1021/jp811468q.
[62] D.S. Bergsman, R.G. Closser, C.J. Tassone, B.M. Clemens, D. Nordlund, S.F. Bent, Effect of backbone chemistry on the structure of polyurea films deposited by molecular layer deposition, Chem. Mater. 29 (2017) 1192–1203, https://doi.org/10.1021/acs.chemmater.6b04530.
[63] R. Ye, Y. Liu, H. Zhang, H. Su, Y. Zhang, L. Xu, R. Hu, R.T.K. Kwok, K.S. Wong, J.W.Y. Lam, W.A. Goddard, B.Z. Tang, Non-conventional fluorescent biogenic and synthetic polymers without aromatic rings, Polym. Chem. 8 (2017) 1722–1727, https://doi.org/10.1039/c7py00154a.
[64] X. Jiang, X. Li, X. Zhu, X.Z. Kong, Preparation of highly uniform polyurea microspheres through precipitation polymerization and their characterization, Ind. Eng. Chem. Res. 55 (2016) 11528–11535, https://doi.org/10.1021/acs.iecr.6b03526.
[65] Y. Feng, H. Yan, F. Ding, T. Bai, Y. Nie, Y. Zhao, W. Feng, B.Z. Tang, Multiring-induced multicolour emission: hyperbranched polysiloxane with silicon bridge for data encryption, Mater. Chem. Front. 4 (2020) 1375–1382, https://doi.org/10.1039/D0QM00075B.
[66] Y. Wang, X. Bin, X. Chen, S. Zheng, Y. Zhang, W. Yuan, Emission and emissive mechanism of nonaromatic oxygen clusters, Macromol. Rapid Commun. 39 (2018) 1800528, https://doi.org/10.1002/marc.201800528.
[67] X. Li, Y. Liao, M. Huang, V. Strong, R.B. Kaner, Ultra-sensitive chemosensors for Fe (III) and explosives based on highly fluorescent oligofluoranthene, Chem. Sci. 4 (2013) 1970–1978, https://doi.org/10.1039/c3sc22107e.
[68] L. Qiu, C. Zhu, H. Chen, M. Hu, W. He, Z. Guo, A turn-on fluorescent Fe^{3+} sensor derived from an anthracene-bearing bisdiene macrocycle and its intracellular imaging application, Chem. Commun. 50 (2014) 4631–4634, https://doi.org/10.1039/c3cc49482a.
[69] G. Song, Y. Lin, Z. Zhu, H. Zheng, J. Qiao, C. He, H. Wang, Strong fluorescence of poly(N-vinylpyrrolidone) and its oxidized hydrolyzate, Macromol. Rapid Commun. 36 (2015) 278–285, https://doi.org/10.1002/marc.201400516.
[70] X. Lin, J. Liu, M. Tian, Y. Bai, Y. Bao, T. Shu, L. Su, X. Zhang, An aggregation-induced phosphorescence-active “turn-off” nanosensor based on ferric-specific quenching of luminescent and water-soluble Au(I)-cysteine nanocomplexes, Anal. Chem. 92 (2020) 6785–6791, https://doi.org/10.1021/acs.analchem.0c01358.
[71] G.L. Long, J.D. Winefordner, Limit of detection: a closer look at the IUPAC definition, Anal. Chem. 55 (1983) 712–724, https://doi.org/10.1021/ac00258a001.
[72] X. Chen, W. Zeng, X. Yang, X. Lu, J. Qu, R. Liu, Thiourea based conjugated polymer fluorescent chemosensor for Cu^+ and its use for the detection of hydrogen peroxide and glucose, Chin. J. Polym. Sci. 34 (2016) 324–331, https://doi.org/10.1007/s10118-016-1760-1.